ACS Medicinal Chemistry Letters

Letter

pubs.acs.org/acsmedchemlett

Structures of Human Acetylcholinesterase Bound to Dihydrotanshinone I and Territrem B Show Peripheral Site Flexibility

Jonah Cheung,*[,†] Ebony N. Gary,[†,∥] Kazuro Shiomi,[‡] and Terrone L. Rosenberry[§]

[†]New York Structural Biology Center, New York, New York 10027, United States

[‡]Kitasato Institute for Life Sciences, Kitasato University, Tokyo 108-8641, Japan

[§]Departments of Neuroscience and Pharmacology, Mayo Clinic Florida, Jacksonville, Florida 32224, United States

Supporting Information

ABSTRACT: Acetylcholinesterase is a critical enzyme that regulates neurotransmission by degrading the neurotransmitter acetylcholine in synapses of the nervous system. It is an important target for both therapeutic drugs that treat Alzheimer's disease and chemical warfare agents that cripple the nervous system and cause death through paralysis. The enzyme has both catalytic and peripheral sites to which inhibitors may bind. Structures of recombinant human acetylcholinesterase in complex with the natural product inhibitors dihydrotanshinone I and territrem B reveal dihydrotanshinone I binding that is specific to only the peripheral site and territrem B binding that spans both sites and distorts the protein backbone in the peripheral site. These inhibitors may function as important molecular templates for therapeutics used for treatment of disease and protection against nerve agents.

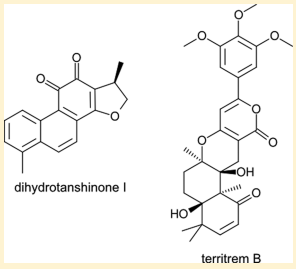

KEYWORDS: *Acetylcholinesterase, dihydrotanshinone I, territrem B, peripheral site, catalytic site, conformational change*

Acetylcholinesterase (AChE) is localized at cholinergic synapses in vertebrates and regulates neurotransmission through rapid hydrolysis of the neurotransmitter acetylcholine into choline and acetate.[1] Drugs that penetrate the blood−brain barrier to inhibit AChE work by increasing levels of acetylcholine to potentiate its physiological effects. Reversible inhibitors of AChE are used to compensate for decreased endogenous acetylcholine levels in the treatment of Alzheimer's disease.[2] More potent irreversible organophosphate (OP) inhibitors completely block AChE activity through covalent modification of the catalytic S203 and have been used as chemical warfare nerve agents that cause death through paralysis from accumulation of acetylcholine in cholinergic synapses.[3] Better insight into inhibitor interaction with AChE may lead to improved therapeutics for treating cholinergic-related diseases or may provide new strategies for protecting against OP poisoning.

The initial structural study of AChE revealed a 20 Å deep active site gorge.[4] The catalytic site is located at the base of the gorge and contains the catalytic triad (H447, E334, and S203 in human AChE). A second or peripheral site extends beyond Y337 (human AChE) at the catalytic/peripheral site interface to the entrance of the gorge and contains numerous aromatic side chains. Kinetic and thermodynamic studies have shown that inhibitors can interact with either or both of the two binding sites in AChE.[5−7] The peripheral site contributes to catalytic efficiency by ensuring that most substrate molecules that collide with and transiently bind to the peripheral site proceed on to the catalytic site.[8,9] It also provides a modest allosteric activation of the acylation step of catalysis with certain bound cationic substrates.[10]

As part of an ongoing effort to develop improved medical countermeasures against OP inactivation of AChE, we are exploring strategies that use peripheral site inhibitors to selectively block the entry of OPs but not acetylcholine. It is therefore necessary to understand the structure−activity relationships (SAR) of ligands specific to the peripheral site, an area of study that has largely been ignored. Higher affinity ligand templates, especially uncharged inhibitors that may be less likely to interfere with entry of cationic acetylcholine, are needed for modification to achieve even greater efficacy and specificity. Natural products that inhibit AChE activity are valuable sources of ligand candidates. Dihydrotanshinone I (DHI) (Figure 1a), a diterpenoid first isolated from the roots of *Salvia miltiorrhiza*,[11] is a relatively high affinity inhibitor of human AChE (K_I = 0.6−0.8 μM[12,13]). Territrem B (TB) (Figure 1a), a fungal meroterpenoid isolated from *Aspergillus terreus*,[14] is an even more potent inhibitor (K_I = 1.7 nM[12]). There are no existing therapeutics based on their scaffolds. A recent investigation using inhibitor competition assays found that DHI binds selectively to the peripheral site, while TB binds to both the catalytic and peripheral sites.[12] In this study, we confirm these results and present high-resolution crystal structures of recombinant human AChE (rhAChE) in complex with DHI and TB. This work elucidates the mechanism of binding of these potential therapeutic drug precursors and reveals conformational changes in the enzyme relevant to future drug design.

Received: August 1, 2013
Accepted: September 23, 2013
Published: September 23, 2013

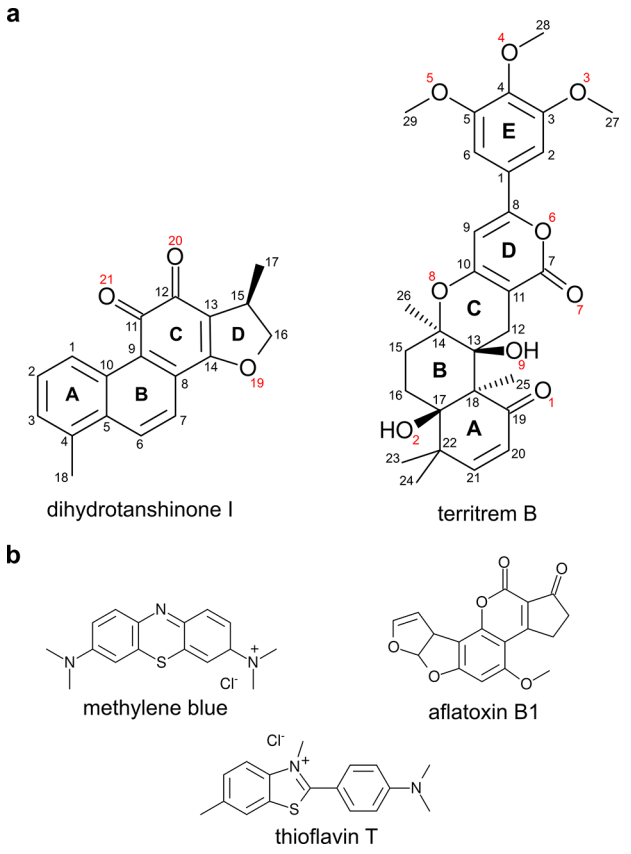

Figure 1. AChE inhibitors. (a) The chemical structures of DHI and TB are shown and labeled with carbon and oxygen numberings in black and red, respectively. (b) Chemical structures of other peripheral site inhibitors discussed in this study.

The structures of rhAChE in complex with DHI and TB are summarized in Table 1. For more detailed data collection and refinement statistics, refer to Supporting Information Table 1. The structure of rhAChE:DHI (Figure 2a) confirms binding of DHI solely within the peripheral site, in an orientation that points the pentacyclic dihydrofuran D-ring (Figure 1a) toward the catalytic site. There are no direct interactions between DHI and residues of the catalytic site. The binding buries 238 Å^2 of solvent-accessible surface area and involves aromatic stacking, hydrogen bond, and hydrophobic interactions.

Table 1. Summary of Structures

	rhAChE:DHI	rhAChE:TB
d_{min} (Å)	2.0	2.3
space group	$P3_121$	$P3_121$
average I/σ_I[a]	9.7 (1.6)	7.7 (1.6)
completeness[a] (%)	99.4 (96.0)	99.6 (100.0)
R_{merge}[a,b] (%)	6.6 (58.7)	8.0 (66.1)
R_{pim}[a,c] (%)	3.7 (34.6)	4.5 (35.0)
R^d/R_{free}[e] (%)	16.0/19.6	17.5/21.1
PDB code	4M0E	4M0F

[a]Values in outermost shell are given in parentheses. [b]$R_{merge} = (\sum|I_i - \langle I_i\rangle|)/\sum|I_i|$, where I_i is the integrated intensity of a given reflection. [c]$R_{pim} = \sum((1/(N-1))^{1/2}(\sum|I_i - \langle I_i\rangle|)/\sum|I_i|$, where I_i is the integrated intensity of a given reflection.[36] [d]$R = \sum||F_o| - |F_c||/\sum|F_o|$, where F_o and F_c denote observed and calculated structure factors, respectively. [e]R_{free} was calculated using 5% of data excluded from refinement.

The planar heteroaromatic A-, B-, and C-rings of DHI form $\pi-\pi$ stacking interactions with the aromatic side chains of W286 and Y341. Carbon atoms of the DHI dihydrofuran D-ring and the attached C17 methyl form hydrophobic van der Waal's contacts with hydrophobic regions of the Y337, F338, Y341, and F297 side chains. Additional hydrophobic contacts are formed between the C18 methyl of the A-ring and side chain atoms of W286 and Y72. The dihydrofuran oxygen (O19) forms a direct hydrogen bond with the Y124 side chain hydroxyl and an indirect hydrogen bond with the D74 side chain, mediated through a water molecule. The same water is also coordinated by the Y341 hydroxyl and is a part of a large water network that extends into the gorge. The two carbonyl oxygen atoms of DHI (O20 and O21 of the C-ring) are involved in hydrogen bonding with the protein backbone, specifically to the amide nitrogen of F295 (direct) and to the carbonyl oxygen of S293 (direct and water-mediated), respectively. Water-mediated hydrogen bonds are also formed between O21 and the S293 side chain hydroxyl and the R296 main chain carbonyl.

The mode of DHI binding revealed in the rhAChE:DHI structure contrasts with that from docking experiments, which predicted deeper binding of the inhibitor in the gorge through a set of different ligand−protein interactions, including direct interaction with the catalytic triad residues S203 and H447.[13] Although the binding of DHI seen in the rhAChE:DHI structure is not within the catalytic site, DHI has been reported to exhibit mixed noncompetitive inhibition.[13] Such inhibition need not arise from direct binding to the catalytic site but can occur because peripheral site inhibitors impose a steric blockade that limits the rates of substrate association with and product dissociation from the catalytic site.[8,15] Thorough SAR studies involving DHI and AChE have not been documented before; however, the IC_{50} values for AChE inhibition by DHI (IC_{50} = 1 μM) relative to that for similar diterpenes, tanshinone I (IC_{50} > 50 μM) and tanshinone IIA (IC_{50} > 140 μM), suggests the importance of the dihydrofuran ring in DHI for high affinity binding.[16] Assuming that tanshinone I and tanshinone IIA bind in a similar manner as DHI, the change of the puckered dihydrofuran ring in DHI (sp3-hybridized C15 center) to a planar furan ring (sp2-hybridized C15 center) in tanshinone I and tanshinone IIA would result in unfavorable steric clash of the attached C17 methyl carbon with the side chains of Y337 and F338, and that would explain the significance of the DHI dihydrofuran ring to improved binding.

Structures of AChE have been solved in complex with other peripheral site ligands such as methylene blue,[17] aflatoxin B1,[18] and thioflavin T,[19] each of which contain 2−3 aromatic rings and are mostly planar in shape like DHI (Figure 1b). These ligands all bind roughly in the same plane and stack between the aromatic side chains of W286 and Y341 (W279 and Y334 in *Torpedo californica* AChE (*Tc*AChE), respectively) through $\pi-\pi$ interactions. Because of the differences in shape and composition of ring substituents, each ligand occupies a different subsite within the peripheral site, and there is only partial overlap of aromatic centers when structures of their complexes are superimposed (Supporting Figure 1a). The binding of each is also coordinated through different hydrogen bonding networks, and it should be noted that the binding of any individual ligand does not fully occupy all available volume

dx.doi.org/10.1021/ml400304w | ACS Med. Chem. Lett. 2013, 4, 1091−1096

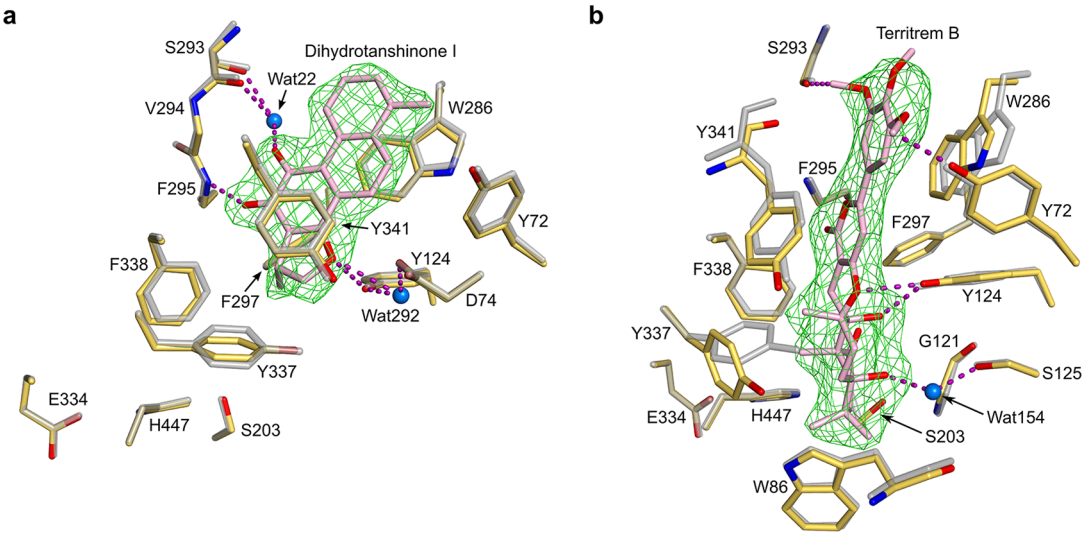

Figure 2. Bound ligands in the rhAChE active site. (a,b) The active site of rhAChE is shown with bound DHI and TB, respectively. Protein and ligand atoms of each complex are shown in stick representation with carbons colored yellow and pink, respectively. Oxygen and nitrogen atoms in the complexes are colored red and blue, respectively. In each panel, residues of the ligand-free state are superimposed and colored gray, waters are shown as turquoise spheres, and hydrogen bonds are depicted as purple dashes. A $F_o - F_c$ simulated-annealing omit map is shown as a green mesh around the ligands, contoured at the 4σ level.

in the peripheral site. This suggests that there is great opportunity for exploratory SAR studies involving these ligands and their chemical derivatives in binding at the peripheral site. One direction of study may involve probing potential interactions with the side chains of residues H287 and E292 that are located at the mouth of the gorge ~7 Å away from DHI as they may provide opportunity for additional coordination of ligand binding.

The binding of TB spans both the catalytic and peripheral sites (Figure 2b) with the A-ring extending into the catalytic site and the E-ring closer to the entrance of the gorge. Unlike the ligands in Figure 1b, the D- and E-rings of TB are not coplanar with DHI when the complexes are superimposed (Supporting Figure 1b). The binding of TB to both the peripheral and catalytic sites involves extensive protein−ligand contacts that bury 444 Å^2 of solvent-accessible surface area. Six ordered water molecules in the active site gorge, seen in the ligand-free rhAChE structure,[20] are displaced upon binding. In the peripheral site, aromatic $\pi-\pi$ stacking interactions are formed between side chains of residues W286 and Y341with the D- and E-rings of TB, respectively. Because of their close proximity, there may be nonclassical CH··O hydrogen bond interactions between the main chain carbonyl of S293 and the side chain hydroxyl of Y72 with the two *ortho*-methoxy substituents on the E-ring. A bifurcated hydrogen bond is formed between the Y124 side chain hydroxyl and the O8 pyranyl oxygen and the O9 hydroxyl of the C-ring near the interface between the peripheral and catalytic sites. The only other apparent hydrogen bond is water-mediated, formed between the side chain of S125 and the O2 hydroxyl of TB in the catalytic site. Interactions in the catalytic site appear to involve stacking interactions between the π-orbitals of the A-ring enone with delocalized orbitals of the protein backbone in residues G120, G121, and G122 of the oxyanion hole. There are also numerous hydrophobic van der Waal's interactions with TB along the length of the gorge. These include contacts between side chains of W86 and H447 and the A-ring in the catalytic site, contacts between the side chain of Y337 and the B-ring at the interface between the catalytic and peripheral sites, contacts involving the side chains of F297 and F338 with the C- and D-rings in the peripheral site, and contacts between Y341 and the E-ring closer to the mouth of the gorge.

Despite difficulties in the synthesis of TB, there are reported SAR studies involving TB, its naturally occurring close analogues, and their synthetic derivatives. Important contributions of the A-ring enone, D-ring pyran-2-one, and aromatic E-ring in binding have been noted,[21−23] and these observations are consistent with the various protein−ligand interactions seen in the structure. Docking studies involving TB have not been successful in predicting the correct mode of binding.[24] However, one of the three predicted binding modes of (+)-arisugacinA,[25] a very close analogue of TB that is expected to bind in the same manner, did closely predict the ligand orientation in the crystal structure. Although it was suggested that covalent modification of AChE by TB may occur through 1,2- or 1,4-addition to the A-ring enone from the catalytic serine side chain hydroxyl,[25] this modification was not supported in the crystal structure. The closest approach between the hydroxyl and the TB A-ring is 3.5 Å (S203 Oγ to TB C20 distance) and formation of a covalent bond there is unlikely. Recent biochemical studies also show reversible binding of TB within the active site gorge,[12] which is more consistent with a noncovalent binding mechanism. The high affinity of TB binding appears to be the result of the combined numerous interactions along the length of the active site gorge.

In comparison to the ligand-free rhAChE structure,[20] there are no major conformational differences in the active site gorge of rhAChE:DHI (all atom root-mean-square deviations (rmsd) = 0.212 Å), and only minor perturbations in some peripheral site side chains (Y337, Y338, and Y341) are seen. In contrast, more significant conformational differences (all atom rmsd = 0.523 Å) are seen with the binding of the bulkier TB. These include a side chain rotation in Y337 that places the aromatic ring closer against the wall of the active site gorge, and a reorientation of the S203 hydroxyl that disrupts the hydrogen bonding network of the catalytic triad. Similar side chain

dx.doi.org/10.1021/ml400304w | *ACS Med. Chem. Lett.* 2013, 4, 1091−1096

rotations are seen in the binding of donepezil to rhAChE,[20] while the binding of donepezil to *Tc*AChE results in side chain rotation only in F330 (equivalent position to Y337 in rhAChE) and not in the active site serine.[26] More striking is that the binding of TB causes significant distortions to contiguous stretches of the protein backbone in the peripheral site and results in an altered gorge shape. One set of motions cause narrowing of the gorge in a direction orthogonal to the plane of bound TB and appears as a qualitative tilt of the C-terminal ends of the $\alpha^3_{6,7}$ and $\alpha^1_{7,8}$ helices closer inward against the ligand (Figure 3). Specifically, the C^α positions of residues

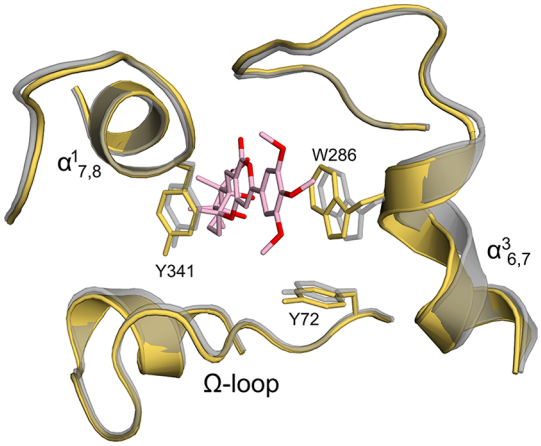

Figure 3. Conformational differences in the peripheral site of the rhAChE:TB complex. Secondary structure elements and a subset of interacting residues in the peripheral site are drawn as ribbons and labeled accordingly. Residues in the TB-bound state and superimposed ligand-free state are colored yellow and semitransparent gray, respectively. Atoms of TB are drawn in stick representation and are colored in the same manner as that in Figure 2.

280−289 and 340−346, which partly form the helices and their C-terminal loops, are shifted by up to 1.5 and 0.9 Å, respectively, in rhAChE:TB. Another set of backbone motions effectively widens the peripheral site in a direction parallel to the plane of bound TB: this set involves residues 72−84 (part of the Ω-loop) and 291−294 in which C^α positions in each segment are displaced by up to 0.5 Å away from the center of the gorge. The need to induce these conformational changes during binding could explain why the association rate constant of TB with rhAChE is unusually low relative to that of other AChE inhibitors.[12]

The active site gorge of AChE is known to have some conformational flexibility. Side chain rotations in the catalytic site and backbone deviations in the nearby acyl-loop result from covalent reaction with OPs.[27−29] The backbone of Y337, W439, and regions of the Ω-loop distort with the binding of huprine W.[30] Binding of bifunctional inhibitors induces rotation of the side chain of W286 (W279 in *Tc*AChE)[31,32] and in some cases significant deviations of the protein backbone,[33] but not in residues of the peripheral site. The set of concerted backbone distortions in the peripheral site caused by TB have not been reported before. Molecular dynamics simulations of AChE suggest that breathing motions alter the dimensions of the active site gorge during catalysis through a range of different conformational states.[34,35] The structure of rhAChE:TB may represent one such state and elucidates dynamic motions in AChE that may occur during catalysis.

In conclusion, both DHI and TB are high affinity inhibitors of AChE that occupy the peripheral site and may serve as precursor compounds for potential therapeutics. As bound TB also extends into the catalytic site, its mechanism of binding involves interactions in addition to those important for the binding of DHI and other planar heteroaromatic inhibitors that bind exclusively to the peripheral site. The modes of binding of these inhibitors within the peripheral site vary to some degree and provide insight for future SAR studies to focus on the peripheral site, a region that warrants more attention. The binding of TB traps the enzyme in a unique conformational state that has not been observed before and illustrates its plastic and dynamic quality even when locked within a crystal lattice. These natural product complexes with AChE reveal important mechanistic details about ligand binding and protein conformational changes that are relevant to future structure-based drug design efforts and computational modeling of drug interaction with acetylcholinesterase.

■ ASSOCIATED CONTENT

Ⓢ Supporting Information

Experimental procedures for cloning, protein expression and purification, crystallization, ligand soaking, data collection, and structure determination and analysis. This material is available free of charge via the Internet at http://pubs.acs.org.

Accession Codes

The structures of the rhAChE:DHI and rhAChE:TB complexes have been deposited in the Protein Data Bank with codes 4M0E and 4M0F, respectively.

■ AUTHOR INFORMATION

Corresponding Author

*(J.C.) Tel: 1-212-939-0660, ext. 9375. E-mail: jcheung@nysbc.org.

Present Address

‖(E.N.G.) Department of Microbiology and Immunology, Drexel University College of Medicine, Philadelphia, Pennsylvania 19104, United States.

Author Contributions

All authors have given approval to the final version of the manuscript.

Funding

Use of the National Synchrotron Light Source, Brookhaven National Laboratory, was supported by the U.S. Department of Energy, Office of Science, Office of Basic Energy Sciences, under contract number DE-AC0298CH10886. This work was supported by the New York Structural Biology Center.

Notes

The authors declare no competing financial interest.

■ ACKNOWLEDGMENTS

We thank Dr. Wayne A. Hendrickson, Dr. Richard Hsung, Dr. Ziyad Al-Rashid, and Dr. Scott A. Wildman for critical reading of the manuscript. We thank Michael J. Rudolph and Matthew C. Franklin for assistance in data collection and scientific discussion. We thank the staff of the X29 beamline at the National Synchrotron Light Source for assistance in data collection.

■ ABBREVIATIONS

AChE, acetylcholinesterase; OP, organophosphate; rhAChE, recombinant human acetylcholinesterase; *Tc*AChE, *Torpedo californica* acetylcholinesterase; DHI, dihydrotanshinone I; TB, territrem B; SAR, structure−activity relationship; rmsd, root-mean-square deviation

■ REFERENCES

(1) Rosenberry, T. L. Quantitative simulation of endplate currents at neuromuscular junctions based on the reaction of acetylcholine with acetylcholine receptor and acetylcholinesterase. *Biophys. J.* **1979**, *26*, 263−289.

(2) Giacobini, E. Cholinesterase inhibitors: from the Calabar bean to Alzheimer therapy. In *Cholinesterases and Cholinesterase Inhibitors. From Molecular Biology to Therapy*; Giacobini, E., Ed.; Martin Dunitz: London, U.K., 2000; pp 181−222.

(3) Millard, C. B.; Broomfield, C. A. Anticholinesterases: medical applications of neurochemical principles. *J. Neurochem.* **1995**, *64*, 1909−1918.

(4) Sussman, J. L.; Harel, M.; Frolow, F.; Oefner, C.; Goldman, A.; Toker, L.; Silman, I. Atomic structure of acetylcholinesterase from *Torpedo californica*: a prototypic acetylcholine-binding protein. *Science* **1991**, *253*, 872−879.

(5) Changeux, J. P. Responses of acetylcholinesterase from *Torpedo marmorata* to salts and curarizing drugs. *Mol. Pharmacol.* **1966**, *2*, 369−392.

(6) Rosenberry, T. L.; Sonoda, L. K.; Dekat, S. E.; Cusack, B.; Johnson, J. L. Analysis of the reaction of carbachol with acetylcholinesterase using thioflavin T as a coupled fluorescence reporter. *Biochemistry* **2008**, *47*, 13056−13063.

(7) Taylor, P.; Lappi, S. Interaction of fluorescence probes with acetylcholinesterase. The site and specificity of propidium binding. *Biochemistry* **1975**, *14*, 1989−1997.

(8) Szegletes, T.; Mallender, W. D.; Thomas, P. J.; Rosenberry, T. L. Substrate binding to the peripheral site of acetylcholinesterase initiates enzymatic catalysis. Substrate inhibition arises as a secondary effect. *Biochemistry* **1999**, *38*, 122−133.

(9) Tara, S.; Elcock, A. H.; Kirchhoff, P. D.; Briggs, J. M.; Radic, Z.; Taylor, P.; McCammon, J. A. Rapid binding of a cationic active site inhibitor to wild type and mutant mouse acetylcholinesterase: brownian dynamics simulation including diffusion in the active site gorge. *Biopolymers* **1998**, *46*, 465−474.

(10) Johnson, J. L.; Cusack, B.; Davies, M. P.; Fauq, A.; Rosenberry, T. L. Unmasking tandem site interaction in human acetylcholinesterase. Substrate activation with a cationic acetanilide substrate. *Biochemistry* **2003**, *42*, 5438−5452.

(11) Li, Z. T.; Yang, B. J.; Ma, G. E. Chemical studies of *Salvia miltiorrhiza* f. alba. *Yao Xue Xue Bao* **1991**, *26*, 209−213.

(12) Beri, V.; Wildman, S. A.; Shiomi, K.; Al-Rashid, Z. F.; Cheung, J.; Rosenberry, T. L. The natural product dihydrotanshinone I provides a prototype for uncharged inhibitors that bind specifically to the acetylcholinesterase peripheral site with nanomolar affinity. *Biochemistry* **2013**, DOI: 10.1021/bi401043w.

(13) Wong, K. K.; Ngo, J. C.; Liu, S.; Lin, H.; Hu, C.; Shaw, P.; Wan, D. C. Interaction study of two diterpenes, cryptotanshinone and dihydrotanshinone, to human acetylcholinesterase and butyrylcholinesterase by molecular docking and kinetic analysis. *Chem. Biol. Interact.* **2010**, *187*, 335−339.

(14) Ling, K. H.; Yang, C. K.; Peng, F. T. Territrems, tremorgenic mycotoxins of *Aspergillus terreus*. *Appl. Environ. Microbiol.* **1979**, *37*, 355−357.

(15) Auletta, J. T.; Johnson, J. L.; Rosenberry, T. L. Molecular basis of inhibition of substrate hydrolysis by a ligand bound to the peripheral site of acetylcholinesterase. *Chem. Biol. Interact.* **2010**, *187*, 135−141.

(16) Ren, Y.; Houghton, P. J.; Hider, R. C.; Howes, M. R. Novel diterpenoid acetylcholinesterase inhibitors from *Salvia miltiorhiza*. *Planta Med.* **2004**, *70*, 201−204.

(17) Paz, A.; Roth, E.; Ashani, Y.; Xu, Y.; Shnyrov, V. L.; Sussman, J. L.; Silman, I.; Weiner, L. Structural and functional characterization of the interaction of the photosensitizing probe methylene blue with *Torpedo californica acetylcholinesterase*. *Protein Sci.* **2012**, *21*, 1138−1152.

(18) Sanson, B.; Colletier, J.; Xu, Y.; Lang, P. T.; Jiang, H.; Silman, I.; Sussman, J. L.; Weik, M. Backdoor opening mechanism in acetylcholinesterase based on X-ray crystallography and molecular dynamics simulations. *Protein Sci.* **2011**, *20*, 1114−1118.

(19) Harel, M.; Sonoda, L. K.; Silman, I.; Sussman, J. L.; Rosenberry, T. L. Crystal structure of thioflavin T bound to the peripheral site of *Torpedo californica* acetylcholinesterase reveals how thioflavin T acts as a sensitive fluorescent reporter of ligand binding to the acylation site. *J. Am. Chem. Soc.* **2008**, *130*, 7856−7861.

(20) Cheung, J.; Rudolph, M. J.; Burshteyn, F.; Cassidy, M. S.; Gary, E. N.; Love, J.; Franklin, M. C.; Height, J. J. Structures of human acetylcholinesterase in complex with pharmacologically important ligands. *J. Med. Chem.* **2012**, *55*, 10282−10286.

(21) Chen, J.; Ling, K. Territrems: naturally occurring specific irreversible inhibitors of acetylcholinesterase. *J. Biomed. Sci.* **1996**, *3*, 54−58.

(22) Jiang, X.; Ao, L.; Zhou, C.; Yang, L.; Zhang, Q.; Li, H.; Sun, L.; Wu, X.; Bai, H.; Zhao, Y. Design, synthesis, and biological evaluation of new territrem B analogues. *Chem. Biodiversity* **2005**, *2*, 557−567.

(23) Peng, F. C. Acetylcholinesterase inhibition by territrem B derivatives. *J. Nat. Prod.* **1995**, *58*, 857−862.

(24) Chen, J. W.; Luo, Y. L.; Hwang, M. J.; Peng, F. C.; Ling, K. H.; Territrem, B. A tremorgenic mycotoxin that inhibits acetylcholinesterase with a noncovalent yet irreversible binding mechanism. *J. Biol. Chem.* **1999**, *274*, 34916−34923.

(25) Al-Rashid, Z. F.; Hsung, R. P. (+)-Arisugacin A: computational evidence of a dual binding site covalent inhibitor of acetylcholinesterase. *Bioorg. Med. Chem. Lett.* **2011**, *21*, 2687−2691.

(26) Kryger, G.; Silman, I.; Sussman, J. L. Structure of acetylcholinesterase complexed with E2020 (Aricept): implications for the design of new anti-Alzheimer drugs. *Structure* **1999**, *7*, 297−307.

(27) Artursson, E.; Andersson, P. O.; Akfur, C.; Linusson, A.; Börjegren, S.; Ekström, F. Catalytic-site conformational equilibrium in nerve-agent adducts of acetylcholinesterase: possible implications for the HI-6 antidote substrate specificity. *Biochem. Pharmacol.* **2013**, *85*, 1389−1397.

(28) Hörnberg, A.; Tunemalm, A.; Ekström, F. Crystal structures of acetylcholinesterase in complex with organophosphorus compounds suggest that the acyl pocket modulates the aging reaction by precluding the formation of the trigonal bipyramidal transition state. *Biochemistry* **2007**, *46*, 4815−4825.

(29) Millard, C. B.; Koellner, G.; Ordentlich, A.; Shafferman, A.; Silman, I.; Sussman, J. L. Reaction products of acetylcholinesterase and VX reaveal a mobile histidine in the catalytic triad. *J. Am. Chem. Soc.* **1999**, *121*, 9883−9884.

(30) Nachon, F.; Carletti, E.; Ronco, C.; Trovaslet, M.; Nicolet, Y.; Jean, L.; Renard, P. Crystal structures of human cholinesterases in complex with huprine W and tacrine: elements of specificity for anti-Alzheimer's drugs targeting acetyl- and butyryl-cholinesterase. *Biochem. J.* **2013**, *453*, 393−399.

(31) Bourne, Y.; Kolb, H. C.; Radić, Z.; Sharpless, K. B.; Taylor, P.; Marchot, P. Freeze-frame inhibitor captures acetylcholinesterase in a unique conformation. *Proc. Natl. Acad. Sci. U.S.A.* **2004**, *101*, 1449−1454.

(32) Colletier, J. P.; Sanson, B.; Nachon, F.; Gabellieri, E.; Fattorusso, C.; Campiani, G.; Weik, M. Conformational flexibility in the peripheral site of *Torpedo californica* acetylcholinesterase revealed by the complex structure with a bifunctional inhibitor. *J. Am. Chem. Soc.* **2006**, *128*, 4526−4527.

(33) Rydberg, E. H.; Brumshtein, B.; Greenblatt, H. M.; Wong, D. M.; Shaya, D.; Williams, L. D.; Carlier, P. R.; Pang, Y.; Silman, I.; Sussman, J. L. Complexes of alkylene-linked tacrine dimers with *Torpedo californica* acetylcholinesterase: binding of Bis5-tacrine

produces a dramatic rearrangement in the active-site gorge. *J. Med. Chem.* **2006**, *49*, 5491−5500.
(34) Shen, T.; Tai, K.; Henchman, R. H.; McCammon, J. A. Molecular dynamics of acetylcholinesterase. *Acc. Chem. Res.* **2002**, *35*, 332−340.
(35) Tai, K.; Shen, T.; Börjesson, U.; Philippopoulos, M.; McCammon, J. A. Analysis of a 10-ns molecular dynamics simulation of mouse acetylcholinesterase. *Biophys. J.* **2001**, *81*, 715−724.
(36) Weiss, M. S. Global indicators of X-ray data quality. *J. Appl. Crystallogr.* **2001**, *34*, 130−135.